Matter waves at a vibrating surface: Transition from quantum-mechanical to classical behavior

J. Felber, R. Gähler, and C. Rausch

Fakultät für Physik E21, Technische Universität München, D-85747 Garching, Germany

R. Golub

Hahn-Meitner-Institut, Glienicker Straße 100, D-14109 Berlin, Germany

We investigate the time-dependent Schrödinger equation for the case of a plane matter wave incident on an oscillating potential step. Approximate solutions are given for different regimes of the problem. The resulting energy spectra are quantized. This may either be interpreted as a phase modulation of the wave or as a coherent multiphonon exchange. A comparison to the results that apply for a beam of classical particles is made. In particular, the transition from the quantum-mechanical to the classical case is examined. We have performed an experiment with very cold neutrons that clearly revealed the discussed effects. Energy splittings of 2.8 to 9.1 neV of the reflected waves were analyzed with an energy resolution of ~1 neV, thus demonstrating the feasibility of such high-resolution experiments with neutron reflectometry.

PACS number(s): 03.75.Be;03.65.−w

I. INTRODUCTION

In recent years several impressive experiments have been performed in the field of neutron optics that elucidate the concept of particle-wave dualism [1]. The diffraction of neutrons by single and double slits or gratings, and the interference of neutrons in interferometers built of gratings or perfect crystals [2] have become so well known that neutron optics is now included in standard textbooks on optics [3].

Due to their low velocities and matter wave frequencies, cold neutrons are also a superb candidate to examine nonstationary interactions of matter waves. This idea was first expressed by Gerasimov and Kazarnovskiĭ in 1976 [4]. Still in 1986, Werner and Klein considered it a future challenge to probe time-dependent interactions with cold neutrons [1].

Up to now only a few nonstationary experiments have been performed in neutron optics. Gähler and Golub for instance, have discussed an experiment where the time-energy uncertainty relation is probed by high-frequency chopping of a neutron beam [5] and experimental work is in progress. Similar problems also were discussed theoretically by Moshinsky [6] and by Nosov and Frank [7]. Badurek *et al.* experimentally demonstrated the time-dependent superposition of spinors [8], and Hamilton *et al.* examined the nonelastic diffraction of neutrons by a surface acoustic wave [9].

We describe a nonstationary experiment that clearly demonstrates the nonclassical, quantized interaction of neutrons with a time-dependent potential. We study the transmission and reflection of very cold neutrons on a mirror that represents a potential step and is excited to a high-frequency oscillation perpendicular to its surface. Although this mirror is of macroscopic dimensions and may thus be regarded as a classical object, analogous to the oscillating magnetic field in magnetic resonance experiments, we will show both in theory and experiment that the resulting interaction with the matter wave is quantized and can be interpreted as a coherent multiphonon exchange. By increasing the amplitude of oscillation we can raise the number of exchanged phonons, approaching eventually a classical behavior. The interest in

such systems is increased by recent suggestions [10] that quantum mechanics might have to be altered in the region between the quantum and classical regimes. However, our work, while demonstrating the transition from quantum to classical behavior, does not address the issue of wave function collapse at the detector.

Hock *et al.* have studied a related problem [11], where the spectral width of a neutron beam, backscattered by a silicon single crystal excited by ultrasound, was examined. However, the spectral resolution was too low to allow the observation of quantized effects. A similar experiment was performed earlier by Klein *et al.*, who measured the time structure—but not the energy spectrum—of a neutron beam that is deflected by a vibrating quartz crystal [12].

The complementary case of the transmission through a potential that is oscillating in height was dealt with by Haavig and Reifenberger [13] and in very recent papers by Summhammer [14] and Frank and Amandzholva [15], but to our knowledge no experiments for this case have been performed until now. A recent quantum-mechanical discussion of the transmission of neutrons through oscillating magnetic fields is given by Golub *et al.* [16], where emphasis is laid on the application to particle beam magnetic resonance and neutron resonance spin echo spectrometers.

In this paper we first discuss the problem of transmission and reflection at a time-dependent potential step theoretically and then present the results of an experiment.

II. DEFINITION OF THE PROBLEM

We consider a one-dimensional potential step of height V_p that moves harmonically as a function of time,

$$V(x,t) = \begin{cases} 0, & x < a(t) \\ V_p, & x \geq a(t) \end{cases} \tag{1}$$

with

$$a(t)=a_0\sin\omega_p t, \quad v_p(t)=\partial a(t)/\partial t=v_p\cos\omega_p t,$$

and

$$v_p=a_0\omega_p \ .$$

We calculate the energy spread that either a classical particle beam or a matter wave approaching the potential step from $x=-\infty$ shows after being transmitted or reflected by the step. A formal solution of the problem of N potential layers, that are time dependent both with respect to position and height, may be found in [17].

Both particle beam and matter wave are assumed to be monochromatic. The initial kinetic energy E_0 corresponds to a (group) velocity of $v_0=(2E_0/m)^{-1/2}$, where m is the mass of the particle. The corresponding wave properties are a matter wave frequency of $\omega_0=E_0/\hbar^1$ and a wave number of $k_0=mv_0/\hbar$.

There is no analytical solution to this problem, either in the classical or in the quantum-mechanical case. However, in certain cases analytical approximations can be found. We will use the following parameters for a classification of these cases: modulation index:

$$\alpha=2k_0a_0, \tag{2a}$$

relative potential height:

$$\beta=V_p/E_0, \tag{2b}$$

relative step velocity:

$$\gamma=v_p/v_0, \tag{2c}$$

relative oscillation frequency:

$$\delta=\omega_p/\omega_0=4\gamma/\alpha. \tag{2d}$$

In the case of a classical particle only two of these parameters (e.g., β, γ) are sufficient for a complete description of the problem. For a matter wave there is one additional degree of freedom and we use either the set (α,β,γ) or (α,β,δ). The meaning of these quantities will be made clearer in the following. We only mention here that $\alpha\ll1$ defines a "high-frequency" and $\gamma\ll1$ a "quasistationary" regime of this problem. The modulation index α, which is proportional to the ratio of the oscillation amplitude and the de Broglie λ_0 $(=2\pi/k_0)$, plays an important role for the transition from quantum-mechanical to classical behavior.

III. SPECTRA FOR A BEAM OF CLASSICAL PARTICLES

In general, a classical particle may pass the potential step several times before it finally escapes the region of oscillation. Therefore its trajectory has to be calculated iteratively.

As an initial condition we assume that the undisturbed trajectory of the particle would reach the origin $x=0$ at t_0. If t_i and v_i denote the time of and the velocity after the ith passing $(i\geqslant0)$, the values after the $(i+1)$th passing are then given by

$$t_{i+1}=t_i+a[\sin\omega_p t_{i+1}-(1-\delta_{0i})\sin\omega_p t_i]/v_i, \tag{3a}$$

$$v_{i+1}/v_0=\begin{cases} -1+2\gamma_{i+1}, & (1-\gamma_{i+1})^2\leqslant-\epsilon\beta \quad (r) \\ \sqrt{(1-\gamma_{i+1})^2+\epsilon\beta}+\gamma_{i+1}, & (1-\gamma_{i+1})^2>-\epsilon\beta \quad (t) \end{cases}$$

$$(3b)$$
$$(3c)$$

with $\gamma_i=v_p(t_i)/v_0$ and $\epsilon=+1(-1)$, if the particle is coming from inside (outside) the potential step. The Kronecker symbol δ_{0i} expresses the initial condition. If (3a) has more than one solution, t_{i+1} takes the value that temporarily succeeds t_i. Equation (3), (r) and (t), describe the velocity after reflection (r) or transmission (t), which is calculated by considering the Doppler shift that occurs during each passage. If $\beta\epsilon>0$ only transmission is possible, because then the particle travels from the side of the higher to the side of the lower potential.

To calculate the energy spectrum of the outgoing beam, one has to determine the different trajectories and with that the final velocities $v_f(t_0)$ as a function of t_0 that occur. As $v_f(t_0)$ has a periodicity of $T_p=2\pi/\omega_p$ it is sufficient to consider only one period, e.g., $t_0\in[0,T_p]$.

The fraction of particle flux $d\Phi$ that is scattered into the interval $[v_f,v_f+dv]$ is proportional to the time dt_0, during which particles arriving at the step are finally scattered to these velocities. The normalized energy spectrum $\varphi^{PB}(E_f)$ of the outgoing particle beam (PB) flux is therefore given by

$$\varphi^{PB}(E_f)=\frac{d\Phi(E_f)}{\Phi_0 dE_f}=\frac{d\Phi(v_f)}{\Phi_0 dv_f}\frac{dv_f}{dE_f}$$

$$=\sum_{branches}\frac{1}{T_p mv_f}\left|\frac{dt_0(v_f)}{dv_f}\right|, \tag{4}$$

where Φ_0 is the incoming flux and $t_0(v_f)$ is the inverse function of $v_f(t_0)$. This inverse is in general not single valued and the right hand side of Eq. (4) has to be summed up over a complete set of branches.

Because Eq. (3a) is implicit, a solution of Eq. (4) can only be found numerically. Here we will only use the results of these calculations when neccessary for comparison with quantum-mechanical results.

A. Quasistationary case

In general the particles can have several collisions, which leads to very rich spectra that are approaching chaotic behav-

---

[1]In this definition of the matter wave frequency we only consider the kinetic energy, thus setting the origin of the energy scale to the neutron's rest mass.

ior [17]. If the relative step velocity is small ($\gamma \ll 1$), and if the beam is either totally reflected (r) or transmitted (t), only one contact with the step occurs (i.e., $v_f = v_1$) and an approximate analytical solution for $\varphi^{PB}(E_f)$ can be given. (As the spectral width of the reflected beam is proportional to γ [cf. Eq. (8)] a sufficient condition for total reflection or transmission is $\gamma \ll |1 - \beta|$.) In this approximation we can set $t_1 \simeq t_0$ in Eqs. (3) and the final velocity v_f is given in first order of γ by a small harmonic modulation

$$v_f(t_0)/v_0 \cong \begin{cases} -1 + 2\gamma\cos\omega_p t_0, & \beta > 1 \quad (r) \\ \sqrt{1-\beta} + \gamma(1-\sqrt{1-\beta})\cos\omega_p t_0, & \beta < 1 \quad (t). \end{cases}$$
(5)

Using Eq. (5) and Eq. (4) we get the approximate spectrum

$$\varphi_{r,t}^{PB}(E_f) \cong \frac{1}{c(E_f)} \left\{ 1 - \left[\frac{1}{\gamma(1-n)} \left(\sqrt{\frac{E_f - V}{E_0}} - |n| \right) \right]^2 \right\}^{-\frac{1}{2}},$$
(6)

with

$$c(E_f) = 2\pi\gamma|1-n|\sqrt{E_0(E_f - V)} ,$$

$$n = \begin{cases} -1 \\ \sqrt{1-\beta} \end{cases}, \quad V = \begin{cases} 0 & (r) \\ V_p & (t) \end{cases}.$$

E_f expresses the total, i.e., the sum of kinetic and potential energy. This spectrum essentially represents the amplitude density of the cosine in Eq. (5). The variable n may be recognized as the index of refraction, i.e., the ratio of the particle velocity (wave number) after and before transmission or reflection. In the latter case, $n = -1$ indicates that the direction of the trajectories is reversed. In this case Eq. (6) just gives the energy spectrum that is produced by the harmonic Doppler drive of neutron backscattering spectrometers [18].

The ranges of final energies in Eq. (6) extend over

$$(E_f - V) \in [E_0[n - \gamma(1 - 1/n)]^2, \ E_0[n + \gamma(1 - 1/n)]^2] .$$
(7)

The spectrum diverges at the borders of this interval. The full width ΔE_f of the spectrum in this approximation is given by $4E_0\gamma|1-n|$, i.e.,

$$\Delta E_f \cong 8\gamma E_0 \quad (r), \quad \Delta E_f \cong 4\gamma E_0|1 - \sqrt{1-\beta}| \quad (t) .$$
(8)

This shows that the energy spread of the reflected beam is higher than that of the transmitted beam unless $\beta < -8$.

IV. SPECTRA FOR A MATTER WAVE

To calculate the energy spectra for an incident matter wave, we have to solve the time-dependent Schrödinger equation for the potential of Eq. (1),

$$i\hbar\frac{\partial}{\partial t}\Psi(x,t) = \left(-\frac{\hbar^2}{2m}\nabla^2 + V(x,t) \right)\Psi(x,t).$$
(9)

As usual in this kind of problem the wave function is separated into three parts,

$$\Psi(x,t) = \begin{cases} \Psi_0(x,t) + \Psi_r(x,t) , & x \leq a(t) \\ \Psi_t(x,t) , & x > a(t) , \end{cases}$$
(10)

where Ψ_0 is the incoming plane wave as defined in Sec. II, and Ψ_r and Ψ_t represent the reflected and transmitted waves, respectively. Compared to the textbook problem of a potential step, the special feature of this problem is of course that the boundary is in motion.

At the boundary $a(t)$ these waves have to satisfy the matching conditions

$$\begin{pmatrix} 1 \\ \partial/\partial x \end{pmatrix}(\Psi_0 + \Psi_r - \Psi_t)|_{(x=a(t),t)} = \begin{pmatrix} 0 \\ 0 \end{pmatrix} .$$

(11a)

(11b)

In analogy to [13,19] this boundary problem can be solved by an ansatz,

$$\Psi_r(x,t) = \sum_n \Psi_{r,n}(x,t) = \sum_n r_n \exp i(-\kappa_n k_0 x - \omega_n t),$$
(12)

$$\Psi_t(x,t) = \sum_n \Psi_{t,n}(x,t) = \sum_n t_n \exp i(\eta_n k_0 x - \omega_n t),$$

with

$$n = 0, \pm 1, \pm 2, \ldots, \quad \omega_n = \omega_0 + n\omega_p = \omega_0(1 + n\delta),$$

$$\kappa_n = \sqrt{\omega_n/\omega_0} = \sqrt{1 + n\delta} ,$$

$$\eta_n = \sqrt{(\omega_n - V_p/\hbar)/\omega_0} = \sqrt{1 + n\delta - \beta} .$$

The variables κ_n and η_n represent the ratio of the wave numbers of the partial waves $\Psi_{(r,t),n}$ and the incoming wave Ψ_0. The change in their wave numbers is not only due to refraction by the potential step, but is also influenced by the shift in energy caused by the oscillation. Therefore we may regard these parameters as "dynamic indices of refraction."

It is obvious from Eq. (12) that the outgoing waves show a discrete line spectrum. The normalized energy spectra of the outgoing (probability) flux of the matter wave (MW) are straightforwardly calculated from Eq. (12),

$$\varphi_{r,t}^{MW}(E_f) = \sum_n \delta(E_0(1 + n\delta) - E_f) \times \begin{cases} |r_n|^2 \text{Re}(\kappa_n) & (r) \\ |t_n|^2 \text{Re}(\eta_n) & (t) \end{cases}$$
(13)

with $\delta(\ )$ representing a Dirac delta function. This is only the time average of the matter wave flux. In addition we call attention to the fact that the outgoing waves Ψ_r and Ψ_t show an interesting bunching effect that is subject to time- and space-dependent collapses and revivals due to the dispersion of the different partial waves in Eq. (12). Of course, only partial waves with real wave numbers, i.e., $E_f > 0$ in the case of Ψ_r and $E_f > V_p$ for Ψ_t, contribute to the flux. This is taken into account by considering only the real part of the dynamical refraction indices.

The amplitudes r_n and t_n are determined by Eq. (11). Making use of Eq. (12) and the relation

$$\exp(iz\sin\theta) = \sum_{m=-\infty}^{+\infty} J_m(z)\exp(im\theta) ,$$
(14)

where $J_m(z)$ is a Bessel function of first kind and mth order, we can rewrite the boundary condition Eq. (11a),

$$\sum_m J_m(a_0 k_0) e^{it(m\omega_p - \omega_0)}$$

$$+ \sum_n \sum_m r_n J_m(-a_0 \kappa_n k_0) e^{it[(m-n)\omega_p - \omega_0]}$$

$$= \sum_n \sum_m t_n J_m(a_0 \eta_n k_0) e^{it[(m-n)\omega_p - \omega_0]}. \quad (15)$$

This equation is only valid for all values of t, if all terms that contain the same time dependence are equal separately. By collecting those terms Eq. (15) can hence be split into a set of equations in which the common and therefore trivial time dependency can be omitted. If we apply the last steps also to Eq. (11b) and use the parameters of Eq. (2), we finally get

$$J_m(\tfrac{1}{2}\alpha) + \sum_n r_n J_{m+n}(-\tfrac{1}{2}\alpha\kappa_n) = \sum_n t_n J_{m+n}(\tfrac{1}{2}\alpha\eta_n),$$
$$(16a)$$

$$J_m(\tfrac{1}{2}\alpha) - \sum_n \kappa_n r_n J_{m+n}(-\tfrac{1}{2}\alpha\kappa_n) = \sum_n \eta_n t_n J_{m+n}(\tfrac{1}{2}\alpha\eta_n),$$

$$\text{with } n,m = 0, \pm 1, \pm 2, \ldots. \quad (16b)$$

The coefficients r_n and t_n are uniquely defined by these equations. However, there is in general no analytical solution to this system of an infinite number of linear equations and we have to look for appropriate approximations.

A. Numerical solution

In general, i.e., if no restrictions are made on the parameters α, β, and δ, only an approximate numerical solution of Eq. (16) is possible.

For every choice of α, β, δ a limit N can be found that makes the contributions of all partial waves Ψ_n with $|n| > N$ negligible within a given tolerance. If the number of partial waves ($|n| \leq N$) and simultaneously the number of equations ($|m| \leq N$) are thus limited, Eq. (16) can be solved with standard numerical methods. The limit N may then be iteratively refined by putting the results for r_n and t_n in Eq. (11) and checking whether the boundary conditions are balanced with sufficient accuracy. If not, the calculations have to be repeated with an enlarged limit N. As can be seen from the following analytical solutions, a starting point may be $N \approx 2\alpha$. We will use the results of such numerical calculations [17] in Sec. V.

B. Small amplitude approximation

In the case of $\alpha \ll 1$, i.e., if the amplitude of the oscillation is small compared with the wavelength of the incident wave, the amplitudes r_n and t_n can be shown to be proportional to $\alpha^{|n|}$ and thus fall off rapidly with rising $|n|$. In first order of α we thus only need to calculate r_n and t_n for $n = -1, 0, +1$.

In an actual experiment it is the maximum velocity of the potential step that is limited by some constraint (in our ex-
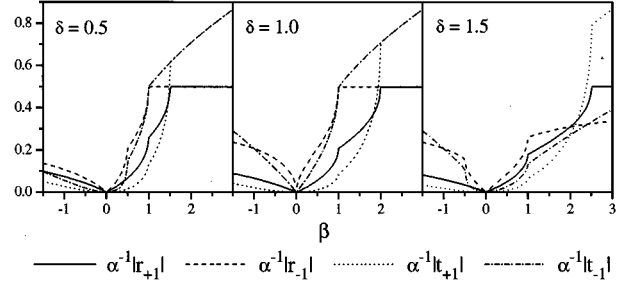

FIG. 1. Amplitudes of the coefficients $r_{\pm 1}$ and $t_{\pm 1}$ as a function of the height of the potential step β and for different oscillation frequencies δ in the case of small modulation $\alpha \ll 1$.

periment the tensile strength of the mirror material). Therefore, in practice, the maximum amplitude α and frequency δ are inversely proportional. This explains why $\alpha \ll 1$ may be called "high-frequency approximation."

By expanding the Bessel functions of Eq. (16) into power series in α and solving the linear equation system for $|n|, |m| \leq 1$, we get

$$r_0 \simeq \frac{1 - \sqrt{1-\beta}}{1 + \sqrt{1-\beta}}, \quad t_0 \simeq \frac{2}{1 + \sqrt{1-\beta}},$$

$$r_{\pm 1} \simeq \pm \frac{\alpha}{2} \frac{1 - \sqrt{1-\beta}}{\sqrt{1 \pm \delta} + \sqrt{1 - \beta \pm \delta}}, \quad (17)$$

$$t_{\pm 1} \simeq \mp \frac{\alpha}{2}(1 - \sqrt{1-\beta}) \frac{\sqrt{1 \pm \delta} - \sqrt{1 - \beta \pm \delta}}{\sqrt{1 \pm \delta} + \sqrt{1 - \beta \pm \delta}}.$$

The terms that have been neglected in these equations are at least a factor of α^2 smaller than the leading ones. The results of Eq. (17) are identical to the first order Born approximation of this problem. As one would expect, the amplitudes r_0 and t_0 in this approximation are the same as for a motionless potential step, which is treated in every textbook on quantum mechanics [20].

Figure 1 shows the dependence of $|r_{\pm 1}|$ and $|t_{\pm 1}|$, both scaled with α^{-1}, on the step height β and the oscillation frequency δ. It is remarkable that the typical critical reflection edges are not only found at $\beta = 1$, as for a motionless step, but also at $\beta = 1 \pm \delta$ ("dynamic critical reflection").

C. Quasistationary case

Consider a motionless potential step of infinite height ($V_p, \beta \to \infty$) at $x = a_0$ and an incident wave Ψ_0 as defined in Sec. II. The reflected and transmitted waves can then immediately be written down:

$$\Psi_r(x,t) = -\exp i[k_0(2a_0 - x) - \omega_0 t], \quad \Psi_t(x,t) = 0. \quad (18)$$

If we now allow for a slow oscillation of the step ($\gamma \ll 1$) we get a rough approximation for Ψ_r by simply replacing a_0 with $a(t) = a_0 \sin\omega_p t$:

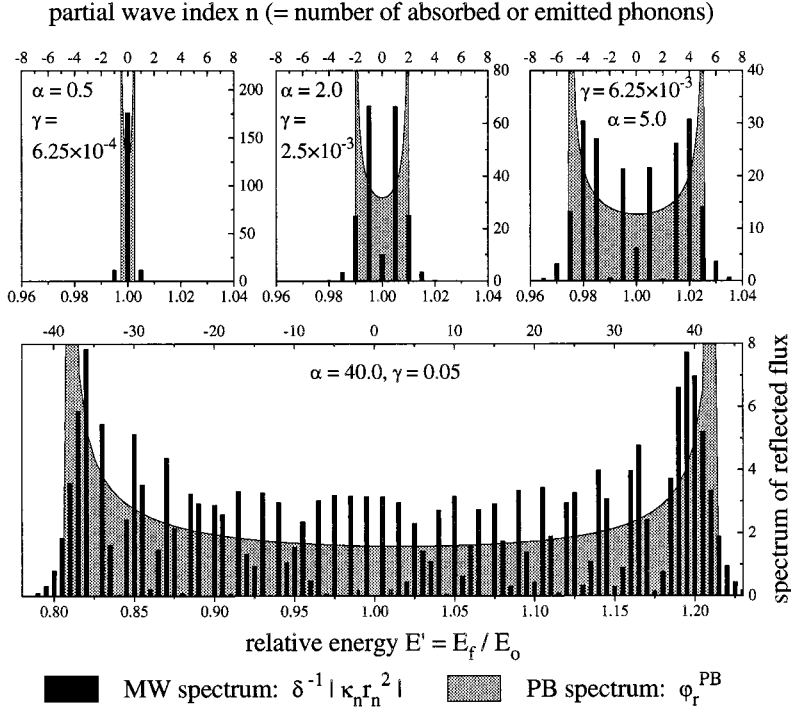partial wave index n (= number of absorbed or emitted phonons)

FIG. 2. Comparison of particle beam and matter wave spectra in the case of total reflection for different values of the modulation index α. The potential height and the oscillation frequency are kept constant ($\beta = 10.0$, $\delta = 0.005$).

$$\Psi_r(x,t) \approx -\exp i(-k_0 x - \omega_0 t + 2a_0 k_0 \sin\omega_p t)$$

$$= -\sum_n J_n(-\alpha)\exp i(-k_0 x - \omega_n t). \qquad (19)$$

The wave function Ψ_t still vanishes. The expression of (19) is no exact solution of the Schrödinger equation because it contains a wrong dispersion relation (k_0 instead of k_n), but this makes no essential difference in the vicinity of the potential step. The term $\alpha\sin\omega_p t$ causes a harmonic phase modulation of Ψ_r with a peak phase shift of α.

From Eq. (16) we can get an approximation with a higher precision that is valid for arbitrary values of β by considering the following.

If the peak velocity of the step is small in relation to the group velocity of the wave ($\gamma \ll 1$), the spectral width of the outgoing waves is also small compared to their mean energy (this can be implicitly proved with the results of the next section [cf. Eq. (21)]). Therefore the dynamic refraction index κ_n varies only weakly as a function of n. This is also true for η_n in the case $|\gamma| \ll |1 - \beta|$. In the complementary case $|\gamma| \approx |1 - \beta|$, i.e., in the vicinity of critical reflection, the absolute values of η_n are small compared to 1, but their relative variation with respect to n is considerable [cf. Eq. (12)]. This is particularly important in the arguments of the Bessel functions in Eq. (16), where η_n is scaled with α which may be substantially larger than 1.

By considering these properties and setting $\kappa_n \approx 1$ outside the Bessel functions arguments Eq. (16) can be transformed to

$$2J_m(\tfrac{1}{2}\alpha) \simeq \sum_n (1 + \eta_n)t_n J_{m+n}(\tfrac{1}{2}\alpha\eta_n) \quad \text{for } (16a)+(16b),$$

$$2\sum_n r_n J_{m+n}(-\tfrac{1}{2}\alpha\kappa_n) \simeq \sum_n (1 - \eta_n)t_n J_{m+n}(\tfrac{1}{2}\alpha\eta_n)$$

for $(16a) - (16b)$.

These equations can be approximately solved by

$$r_n \simeq \rho_n J_n(-\tfrac{1}{2}\alpha(1 + \kappa_n)) , \quad \rho_n = \frac{1 - \eta_n}{1 + \eta_n},$$

$$t_n \simeq \tau_n J_n(\tfrac{1}{2}\alpha(\eta_n - 1)) , \quad \tau_n = \frac{2}{1 + \eta_n} . \qquad (20)$$

In the case $\beta \to \infty$, also $|\eta_n| \to \infty$ and $r_n \to -J_n(-\tfrac{1}{2}\alpha(1 + \kappa_n)) \approx -J_n(-\alpha)$, thus reproducing the result of Eq. (19). An examination of the precision of Eqs. (20) reveals that the relative error of r_n and t_n, and coupled to these also the error of the balance of Eq. (11), is of the order of γ but rises to about $\sqrt{\gamma}$ near critical reflection ($\beta \approx 1$), whereas α has no important influence on the precision.] The factors ρ_n and τ_n represent the stationary reflection and transmission coefficients of the partial waves $\Psi_{r,n}$ and $\Psi_{t,n}$, i.e., they are equal to the ratio of the amplitudes of the outgoing and the incident wave in the case of the reflection of a matter wave of energy $\hbar\omega_n$ by a motionless potential step.

V. DISCUSSION

First we discuss the influence of the modulation index α, keeping the height of the potential step at a high value ($\beta = 10$) to ensure nearly complete reflection and the frequency of the oscillation low ($\delta = 5 \times 10^{-3}$). The peak velocity of the step is then proportional to α ($\gamma = \delta\alpha/4 = 1.25 \times 10^{-3}\alpha$). In Fig. 2 we compare the continuous energy spectra of a particle beam of Eq. (6) with the

line spectra of a matter wave of Eq. (20). The latter are shown as an appropriate scaled ($\times \delta^{-1}$) histogram of the relative weights of the δ functions in Eq. (13). For the chosen value of β only a negligible portion of the MW transmits (none of the PB) and we only consider the reflected flux.

From Fig. 2 we can see that the MW spectra consist of roughly 2α lines, thus explaining the reference to α as modulation index. This can also be proved with Eq. (20) and the property of the Bessel functions that $J_n(\alpha)$ vanishes rapidly with rising $|n|$, if $|n| > |\alpha|$ and α is real. By multiplying the number of excited harmonics with their distance in energy, we can calculate the typical width of the MW spectra,

$$\Delta E_r^{MW} \simeq 2\alpha\hbar\omega_p = 2\alpha\,\delta E_0 = 8\gamma E_0,$$

$$\Delta E_t^{MW} \simeq \alpha|\eta_0 - 1|\hbar\omega_p = \alpha\delta|\eta_0 - 1|\gamma E_0 \qquad (21)$$

$$= 4\gamma|1 - \sqrt{1-\beta}|E_0.$$

The expression for ΔE_t^{MW} is calculated in the case that the spectrum of the transmitted wave essentially lies above the potential step, which happens for $|\gamma| \ll 1 - \beta$; the case of a partially evanescent transmitted wave is treated later. The spectral widths are in accordance with Eq. (8), with the difference that for a PB the range of final energies is sharply limited, whereas for a MW any harmonic ω_n can be found in the outgoing waves, its amplitude, however, vanishing rapidly outside the range of Eq. (21).

It should be emphasized that the portion of the MW spectra that lies outside the limits of the classical spectra given by Eq. (8) can in no way be understood classically: The velocities of those particles are (much) faster or slower than is permissible from the classical point of view.

The modulation index α plays an important role in the transition of the MW to the PB spectra, i.e., from the quantum-mechanical to the classical case: For low values of α ($\alpha < 1$) the spectrum of the reflected MW contains only a few strong harmonics and is therefore, apart from their comparable mean widths, quite different than the PB case. This difference partially vanishes when α rises, because then the spectrum of the PB asymptotically coincides with the mean envelope of the lines of the MW spectrum. However, even if α approaches infinity the intensities of the lines fluctuate from zero to about twice the value of the PB flux distribution (cf. Fig. 2, $\alpha = 40$). The effect that oscillations appear during the approach to the classical limit has been discussed by Peres [21].

One way to complete the transition from the quantum-mechanical to the classical case, i.e., to get rid of these fluctuations and change the line spectra to continuous ones, is to start, in addition to letting α go to infinity, with an incident beam of wave packets instead of a plane wave. The spectra of the outgoing waves in this case are calculated by convolving Eq. (13) with the energy distribution of the incident packets. If the mean width of this distribution ΔE_0^{MW} exceeds the line spacing δE_0, the line spectrum characteristic is washed out and both cases, PB and MW, coincide asymptotically.

The spectra would be equally smeared out if we start with an incoherent polychromatic mixture of plane waves instead of coherent wave packets. In our experiment we actually did not prepare wave packets (e.g., by using a chopper), but we only limited the incident spectrum well enough to ensure the visibility of the spectral lines. A difference between those two cases might only be visible in the time dependence of the outgoing matter wave, but unfortunately such effects seem not to be observable in our experimental setup.

This transition from quantum-mechanical to classical spectra may also be interpreted from first principles: To provide the wave packets with classical behavior we have to demand that the time Δt_{pass} that it takes a packet to pass the step is small compared to the oscillation period of the step

$$\Delta t_{pass} \ll T_p = 2\pi / \omega_p,$$

because only then are the instant of passage and the momentary velocity of the step is defined well enough to allow the calculation of a classical Doppler shift. If we consider the time-energy uncertainty relation this is only possible if

$$\Delta E_0^{MW} \gg \hbar / \Delta t_{pass} \gg \hbar / T_p = \delta E_0 / 2\pi.$$

Next we discuss the influence of the step height on the spectra. Figure 3 shows a comparison of the dependence of the PB and the MW spectra on β, calculated by numerical solutions of Eq. (3) and Eq. (16). To be able to display the complete wave functions (including the evanescent partial waves) we have plotted the expressions $|\kappa_n r_n^2|$ and $|\eta_n t_n^2|$ that differ from the actual fluxes in Eq. (13) only if κ_n or η_n is imaginary.

The MW flux is for all values of β split into a reflected and transmitted portion, whereas for the PB splitting occurs only around $\beta \approx 1$.

The PB results in Fig. 3 clearly reveal the difference of the spectral widths with respect to reflection or transmission according to Eq. (8). This is also true for the MW in the case of $\beta = 0.5$. For $\lesssim 1$, however, the transmitted partial waves that have imaginary wave numbers ($\hbar\omega_n < V_p$) and thus are evanescent, show a substantial growth with rising β. This can be explained with Eq. (20) and the exponential growth that Bessel functions show when continued for complex arguments.

This behavior has no severe consequences as these partial waves carry no flux. In addition, it can be shown that due to their alternating phases these partial waves extinguish one another in the summation of Eq. (12) and the total transmitted wave function Ψ_t vanishes in the case $\beta \to \infty$.

Another property of the flux spectra is their asymmetry with respect to energy gain or loss (cf. Fig. 3, $\beta = 1.5$). If we define an effective modulation index $\alpha_{r,n}^{eff} = \frac{1}{2}\alpha(1 + \kappa_n)$ it is obvious from Eqs. (17) and (20) that the upscattered partial waves ($n > 0$) are subject to a higher effective phase modulation due to their increased wave numbers and that this part of the spectrum extends to higher values of $|n|$. On the other hand, partial waves with higher energies are reflected less, which is expressed by ρ_n in Eq. (20). Thus the amplitudes of the upscattered harmonics are, on the average, smaller than the downscattered ones. A more detailed survey reveals that the first effect is dominating and that the mean energy is increased after passing the oscillating step.

Up to now we have discussed the MW spectra in terms of simultaneous phase and amplitude modulations. The phase modulation is caused by the motion of the step, and the amplitude modulation is due to the different reflection and
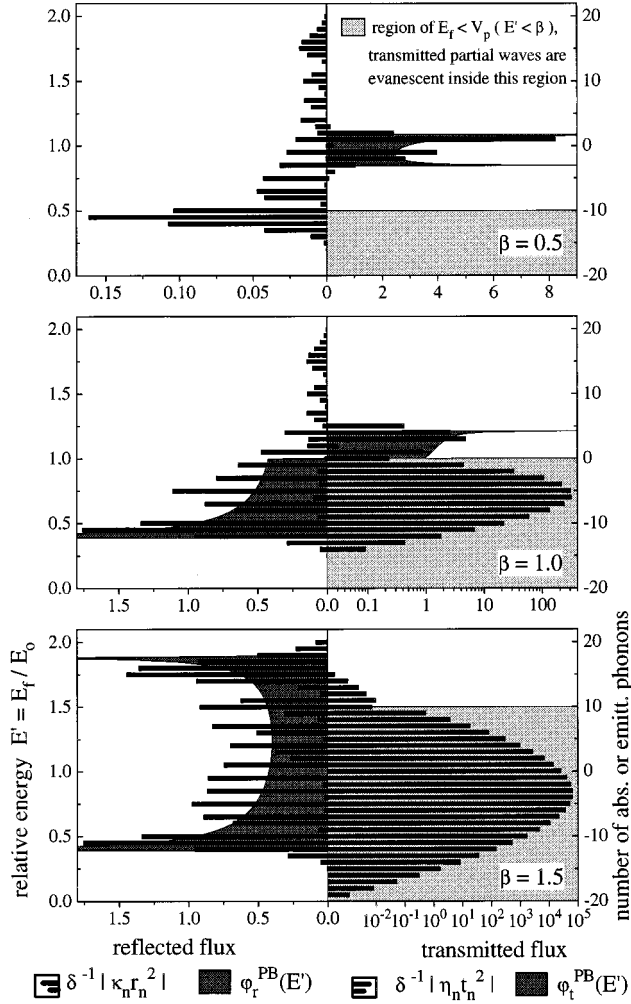
FIG. 3. Comparison of particle beam and matter wave spectra in the vicinity of critical reflection for different values of the step height β ($\alpha = 15.0$, $\delta = 0.05$, $\gamma = 0.1875$ kept constant). The reflected and transmitted flux spectra are plotted to the left and right, respectively. The histograms give the results of the quantum-mechanical calculations, while the dark shaded areas represent the classical spectra. The light shaded areas represent the potential step. On the left ordinate the final relative energy is shown. The right one gives the corresponding number of exchanged phonons.

transmission indices that the distinct partial waves are subject to. The discreteness of the spectra results from the periodicity of these modulations.

Another possible interpretation is to regard the wave functions of Eq. (12) as coherent superpositions of partial waves Ψ_n that have absorbed or emitted n phonons at the potential step. This interpretation is emphasized in our experiment, where the incidence of the matter wave is not perpendicular to the potential step, which leads to a splitting of the partial waves not only in energy but also with respect to the outgoing direction. In consequence, suggestions have been made to use this effect for coherent beam splitting in interferometry with neutrons [22] and atomic beams [23].

In our case the oscillation of the step is described by a well defined oscillation amplitude. Thus the step is not in an eigenstate of the phonon number, but has to be modeled as
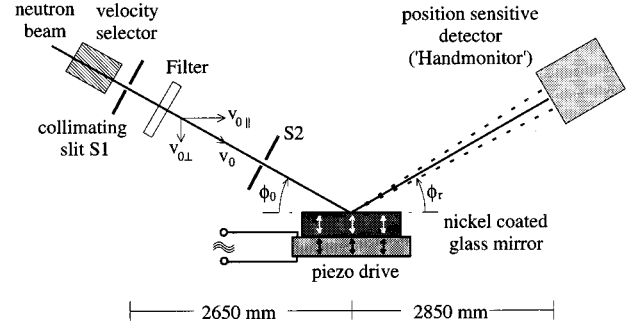

FIG. 4. Schematic experimental setup.

an appropriate superposition of states with different occupation numbers. Indeed, the mean occupation number is very high in our experiment (roughly 10^{24} phonons), so the mirror that represents the potential step in the experiment is really in a highly classical state.

VI. EXPERIMENT WITH VERY COLD NEUTRONS

We performed an experiment to demonstrate some of the results of the previous sections. The measurements were made at the research reactors of Munich and Geesthacht (FRM and FRG). Here we only describe the basic setup of the experiment, details can be found in [17].

Figure 4 shows the schematic setup. A beam of very cold neutrons (VCN) with a mean wavelength of 24 Å is reflected by a mirror that is excited to an oscillation perpendicular to its surface by a piezo drive. The resulting energy spectrum is analyzed by determining the profile of the outgoing beam.

To set up an experiment with a one to one correspondence to the discussed one-dimensional problem one would have to use ultracold neutrons (UCN) because their energies (<300 neV) are comparable to the mean Fermi pseudopotential of most materials, thus allowing a perpendicular incidence on a surface that represents the potential step.

However, due to intensity arguments and the large sample sizes that would be necessary in UCN experiments it is easier to use VCN ($E_0 \approx 100$ μeV) under grazing incidence. In this case we can bring the experiment into coincidence with the one-dimensional problem by transforming to a reference frame that is moving with $-v_{0\parallel}$ (cf. Fig. 4 for a definition of involved quantities). In consequence we have to replace the quantities in Eq. (2) by the perpendicular components of their analogs in the experiment.

An energy transfer of $\Delta E_\perp$ by the mirror that changes only the perpendicular velocity component of the neutrons causes a beam deflection of

$$\tan\phi_r = \frac{v_{r\perp}}{v_{0\parallel}} = \tan\phi_0 \sqrt{1 + \frac{\Delta E_\perp}{E_{0\perp}}}, \qquad (22)$$

where $E_{0\perp} = E_0 \sin^2\phi_0$ is the "perpendicular" energy component of the incident beam.

Because ϕ_0 and $\Delta E_\perp$ are relatively small in our setup, we can linearize

$$\Delta\phi = \phi_r - \phi_0 \simeq \frac{\Delta E_\perp}{m_n v_0 v_{0\perp}} \; , \qquad (23)$$

where m_n is the neutron mass.

The mirror that was used in the experiment was a disk (4 mm thickness $\times$ 40 mm diameter) of nickel coated glass (layer thickness $\approx$ 200 nm). We kept $v_{0\perp}$ (≈ 5.7 m/s) of the beam well below the critical velocity of nickel ($v_{crit} \approx 6.7$ m/s) to ensure total reflection. The mirror was mounted on a piezo ceramic transducer (lead zircon titanate, 3 mm $\times$ 50 mm diameter). The thicknesses of both disks were chosen to match their acoustic resonances. We used two different thickness resonance modes: the fundamental mode at 693 kHz, that allowed higher amplitudes, and its third harmonic at 2.22 MHz, that produced a higher line separation at the expense of reduced amplitudes.

To prevent a spreading of the reflected beam the mirror has to be sufficiently planar. This becomes a problem when vibrations are excited, because then a curving of the surface arises due to thermal tensions caused by dissipative heating. We observed the mirror's flatness *in situ* by an autocollimation telescope and applied appropriate cooling by compressed air. The piezo disk was excited in series resonance by means of a crystal stabilized sine wave generator and an impedance matching network. To calibrate the ultrasound amplitude with respect to the applied power and determine the modal structure of the oscillation we built a special light interferometer of Michelson type and scanned the mirror surface. The measurements showed a strong coupling of thickness and higher harmonics radial modes which results in a structure of concentric areas of minimum and maximum amplitudes. We applied a special edge beveling technique [24,25] to suppress this coupling and to produce a pistonlike motion, which also raised the quality factor of the resonances and thus reduced heating of the sample. With optimum beveling the width of the surface amplitude distribution was about 25% full width at half maximum (FWHM). This inhomogeneity was sufficiently low to neglect beam deflection due to the dynamic curving of the mirror surface, but had to be considered in the comparison of experiment and theory by averaging over adequate distributions of α.

Evaluating Eq. (23) with the experimental parameters we can estimate the angular separation of two lines to be about 3×10^{-4} rad in the case of the fundamental resonance (693 kHz), corresponding to a spatial distance of about 0.8 mm at the detector plane. To resolve this minute deflection we restricted the beam divergence in the direction perpendicular to the mirror by means of two slits to values of about $(1.8-4.1) \times 10^{-4}$ rad, depending on which mode we examined. The beam divergence perpendicular to the plane of Fig. 4 does not degrade the resolution and we used a neutron guide (two parallel pieces of nickel coated glass separated 25 mm) for intensity gain.

From Eq. (23) it is obvious that $\Delta\phi$ depends on v_0, i.e., the resolution is decreased by the velocity spread of the incident beam. To get rid of this effect, which would have been visible when using the full spectrum of the neutron guide that was defined to about 10% ($\Delta v/v$) by a velocity selector, we used an additional filter that was set to a bandwidth of about 2%. The filter uses a successive transmission and reflection by mirrors that were optimized for a steep cutoff at
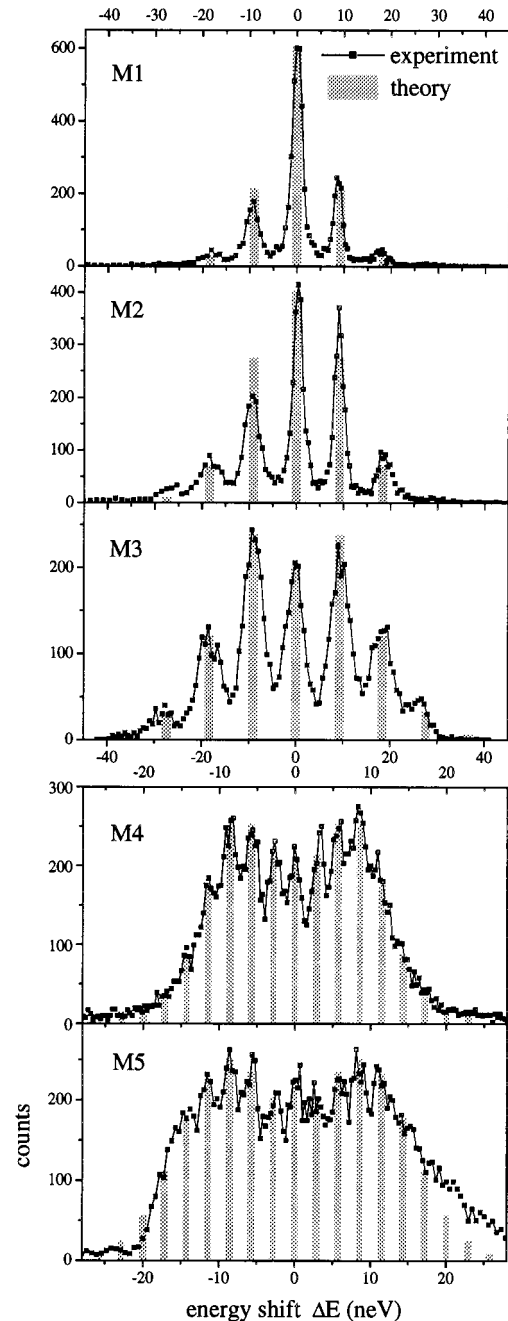

FIG. 5. Results of the experiment in comparison to the theory. The value of the modulation index α is increased from M1 to M5 (cf. Table I for experimental parameters).

critical reflection and are slightly tilted with respect to each other to tune the bandwidth (see [17] for details).

We were able to increase the efficiency of the measurement with respect to the usual method of scanning a narrow slit by using a recently developed two-dimensional position sensitive detector (PSD) [26]. This PSD is distinguished by a superb resolution (about $35 \times 35 \; \mu m^2$), a high efficiency of about 90% at 24 Å, and a high noise and γ-ray immunity—no background was subtracted in the measurements shown in Fig. 5 although the neutron count rate was only a few neutrons per second or less. The measurements

TABLE I. Experimental parameters.

Angle of incidence: $\phi_0 = 2.00°$				
Velocity:	$v_0 = 164 \pm 3$ m/s,	$v_\perp = 5.71 \pm 0.11$ m/s		
Mean energy:	$E_0 = 140$ μeV	$E_\perp = 171$ neV		
Potential height:	$V_p = 235$ neV	$\beta = 1.37$		
Measurement	M1	M2	M3	M4	M5
Frequency (δ)	2.2206 MHz (0.0538)			692.95 kHz (0.0167)	
Mean amplitude (nm)	5.3	8.0	10.9	23.2	32.1
α	0.95	1.45	1.98	4.21	5.82
γ	0.013	0.020	0.027	0.018	0.024

were carried out using the detector only as a one-dimensional PSD by summing up all counts in columns perpendicular to the plane of Fig. 4.

VII. EXPERIMENTAL RESULTS

In Fig. 5 the results of different measurements are shown by plotting the neutron counts in each detector column versus the energy transfer that was calculated from the beam deflection according to Eq. (22). These measurements are compared to what is expected from theory (shaded histograms). The relevant experimental parameters of the different measurements are listed in Table I. Each data point corresponds to a spatial distance of about 0.2 mm (0.1 mm in the case of M4 and M5) at the detector plane.

The measurements clearly show that the beam profiles consist of several peaks, thus proving the quantization of the energy transfer by the oscillating mirror. The width of the single peaks can be fully explained by the experimental resolution, thus they conform to the assumption that the transferred energy spectrum is discrete. The position of the peaks is in close agreement with what is expected from theory.

This is also true for the typical excitation pattern of the sidebands as a function of α. However, the surface inhomogeneity of the mirror oscillation has to be considered by averaging the theory spectra calculated from Eq. (20) over appropriate distribution of α. The width $\Delta\alpha$ and shape of these distributions was deduced from the optical measurement of the surface modes. This averaging degrades the visibility of the strong modulation of the intensities of neighboring sidebands that shows in the theoretical results in Figs. 2 and 3.

We have made least-squares fits for a quantitative comparison of experiment and theory. In addition to the distribution of α, the finite resolution caused by the beam divergence and the incident beam velocity spectrum were taken into concern. The fitting parameters were α, δ, and $\Delta\alpha$.

The results of the fit showed a close agreement of theory and experiment. The relative deviation of α and $\Delta\alpha$ was on the order of 5%. The main errors in these parameters came from ambiguities in the optical determination of the oscillation amplitudes. The parameter δ, i.e., the separation of the distinct lines of the energy spectra is not influenced by these errors. Indeed, we found an excellent agreement of the values of δ that we got from the neutron experiment compared to its expected values calculated from the frequencies that

were applied to the mirror: The fit gave a line spacing (phonon energy) of $\Delta E_\perp = 2.864 \pm 0.011$ (1σ) neV for the 693 kHz mode which is to be compared with $\hbar\omega_p = 2.866$ neV, and 9.16 ± 0.05 neV for the 2.22 MHz mode, whose theoretical value is 9.18 neV.

VIII. CONCLUSIONS

We have discussed the problem of the reflection and transmission of a particle by an oscillating potential step. We present both classical and quantum-mechanical calculations. The classical model is expected to be valid in the region where the vibration amplitude is large compared to the particle wavelength, and shows a very rich behavior approaching that of chaotic systems in the region of parameter space where the particles can make several collisions (see [17] for details).

The quantum-mechanical calculations show that with small vibration amplitudes the energy of the reflected neutrons is changed by $\pm\hbar\omega_p$ (one phonon exchange). As the amplitude increases, one sees additional sidebands corresponding to two and higher numbers of phonons. Eventually the spectrum of the reflected neutrons approaches that of a classical particle. As mentioned above in Sec. V and has been discussed by Peres [21], the classical limit only arises by neglecting or averaging the oscillations which appear as one takes the quantum-mechanical calculations to the limit. In practice these oscillations are always eventually averaged by the finite experimental resolution.

We have presented the results of a series of experiments where very cold neutrons are reflected from a glass surface which was vibrated by a piezoelectric transducer. Our measurements were able to span the parameter region corresponding to both one phonon and multiphonon (approximately ± 12) exchange. Although we have not yet been able to go into the strong classical limit, we see clearly the approach to the spectrum expected classically. The results are in all cases compatible with the quantum-mechanical description whose validity is clearly a function of the experimental resolution.

Thus in this system we can observe a continuous transition from quantum (few phonon exchange) to classical (many phonon exchange) behavior by simply adjusting an experimental parameter.

ACKNOWLEDGMENTS

[1] See, e.g., S. A. Werner and A. G. Klein, in *Methods of Experimental Physics*, edited by K. Sköld and D. L. Price (Academic Press, New York, 1986), Vol. 23, Part A.

[2] See, e.g., V. F. Sears, *Neutron Optics* (Oxford University Press, New York, 1989).

[3] H. Rauch, in *Bergmann-Schaefer, Band 3: Optik*, edited by H. Niedrig (de Gruyter, Berlin, 1993).

[4] A. S. Gerasimov and M. V. Kazarnovskiĭ, Zh. Éksp. Teor. Fiz. **71**, 1700 (1976) [Sov. Phys. JETP **44**, 892 (1976)].

[5] R. Gähler and R. Golub, Z. Phys. B **56**, 5 (1984); J. Phys. (Paris) Colloq. **45**, C3-229 (1984); J. Felber *et al.*, Physica B **162**, 191 (1990).

[6] M. Moshinsky, Phys. Rev. **88**, 625 (1952).

[7] V. G. Nosov and A. I. Frank, J. Moscow Phys. Soc. **1**, 1 (1991); Phys. Lett. A **188**, 120 (1994); Phys. At. Nucl. **57**, 968 (1994).

[8] G. Badurek, H. Rauch, and D. Tuppinger, Phys. Rev. A **34**, 2600 (1986).

[9] W. A. Hamilton *et al.*, Phys. Rev. Lett. **58**, 2770 (1987).

[10] There is a large body of literature on this issue. See, e.g., the articles by O. Penrose, E. J. Squires, L. Diósi, P. Pearle, and G. C. Ghirardi in *Quantum Chaos—Quantum Measurement*, Vol. 158 of *NATO Advanced Study Institute, Series B: Physics*, edited by P. Cvitanović, I. Percival, and A. Wirzba (Plenum, New York, 1992), and for a more popular treatment see R. Penrose, *The Emperor's New Mind* (Oxford University Press, New York, 1989).

[11] R. Hock *et al.*, Z. Phys. B **90**, 143 (1993).

[12] A. G. Klein *et al.*, Appl. Phys. Lett. **10**, 294 (1967).

[13] D. L. Haavig and R. Reifenberger, Phys. Rev. B **26**, 6408 (1982).

[14] J. Summhammer, Phys. Rev. A **47**, 556 (1993).

[15] A. I. Frank and D. B. Amandzholva (unpublished).

[16] R. Golub, R. Gähler, and T. Keller, Am. J. Phys. **62**, 779 (1994).

[17] J. Felber, Ph.D. thesis, Technische Universität München, 1994.

[18] See, e.g., M. Bée, *Quasielasic Neutron Scattering*, (Adam Hilger, London, 1988), Sec. 3.3.

[19] J. H. Shirley, Phys. Rev. **138**, 979 (1965).

[20] See, e.g., L. D. Landau and E. M. Lifschitz, *Lehrbuch der theoretischen Physik, Band III: Quantenmechanik* (Akademie Verlag, Berlin, 1971), p. 83.

[21] A. Peres, in *Quantum Chaos—Quantum Measurement*, Vol. 158 of *NATO Advanced Study Institute, Series B: Physics*, edited by P. Cvitanović, I. Percival, and A. Wirzba (Plenum, New York, 1992), p. 249.

[22] R. Golub and S. K. Lamoreaux, Phys. Lett. A **162**, 122 (1992).

[23] C. Henkel *et al.*, in *Optics and Interferometry with Atoms*, Special issue of J. Phys. (France) II **4**, 1877 (1994).

[24] R. Bechmann, J. Sci. Instrum. **29**, 73 (1952).

[25] E. A. G. Shaw, J. Acoust. Soc. Am. **28**, 38 (1956).

[26] C. Rausch *et al.*, SPIE **1737**, 255 (1992); J. Neutron Res. (to be published).